Next generation 50G PON flexible transmitters based on directly modulated VCSELs

Paola Parolari
Dip. Elettronica Informazione e Bioingegneria
Politecnico di Milano
Milano, Italy
paola.parolari@polimi.it

Alberto Gatto
Dip. Elettronica Informazione e Bioingegneria
Politecnico di Milano
Milano, Italy
alberto.gatto@polimi.it

Christian Neumeyr
Vertilas GmbH
Garching, Germany
neumeyr@vertilas.com

Pierpaolo Boffi
Dip. Elettronica, Informazione e Bioingegneria
Politecnico di Milano
Milano, Italy
pierpaolo.boffi@polimi.it

***Abstract*— We consider long-wavelength vertical cavity surface emitting lasers (VCSELs) directly modulated with discrete multitone (DMT) signals as a very promising solution for implementing energy-efficient transmitters for 50G passive optical networks (PONs). Two scenarios based on single sideband and dual sideband modulation are taken into account. Preliminary experimentation with already available short-cavity VCSELs operating in the third window is presented to show the PON performance as a function of the accumulated chromatic dispersion and of the received power. Experimental results are also used to validate a simulation tool, which is further used to provide the performance evaluation of transmitters based on next-generation short cavity VCSELs with higher bandwidth (up to 20 GHz), operating in the O band. Thanks to its water-filling nature, DMT is demonstrated to enable PON flexibility: in fact, considering the statistics regarding a commercially deployed PON, a significant increase of the maximum aggregated capacity is provided, optimizing the PON resource usage with respect to the losses and dispersion impairments.**

Keywords—Passive optical networks, Flexible modulation, VCSEL, DMT, access.

I. Introduction

The optical access networks are almost exclusively represented by passive optical networks (PONs), whose deployment, in 2019, has actually exceeded 500 million served homes [1]. The time division multiplexed passive optical networks (TDM-PON) based on point-to-multipoint passive optical power splitters in the outside distribution network (ODN) are the most commonly optical access network architectures deployed so far. NG-PON2 standard tried to satisfy the continuous growth of bandwidth demand, pushing from the core network, with the introduction of the wavelength variable, offering 80 Gb/s capacity with a Time and Wavelength Multiplexed- passive optical network (TWDM-PON), and 240 Gb/s if 16 point-to-point WDM channels are added [2]. However, the costs and technological challenges of burst-mode, tunable optical network units (ONUs) have not slacked off in these years and thus it will be unlikely that TWDM-PON would ever be a fiber to the home (FTTH) solution [1].

To satisfy the bandwidth (BW) demand of new high BW applications, the line rate increase beyond the 10 Gb/s seems the preferred solution. Actually, after the work on the standardization of 25G TDM-PON, IEEE and ITU are looking for the candidate modulation formats and technologies for the next 50-Gbit/s PON (50G-PON) [3]. As the success of previous generations of TDM-PONs has relied on the pre-existence of mature high-volume technologies, a natural choice would be to follow the IEEE 802.3bs 50-Gb/s lane standardization for data center intra-connect (DCI). However, PON links need to address much higher power budget and longer reaches (up to 20-40 km) with respect to point-to-point DCI optical links, thus alternative solutions should be evaluated [3].

Discrete multi-tone (DMT) is a promising technique which allows the use of low-bandwidth optical components to achieve high capacity, even maintaining the cost-effective intensity modulation/ direct detection (IM/DD) approach [4]. DMT allows the exploitation of low cost, low power consumption devices, as vertical-cavity surface-emitting lasers (VCSELs), in the transceivers. Recently, we have proposed to use a DMT directly modulated (DM) tunable VCSEL to achieve a colorless ONU transmitter, targeting a transported upstream (US) capacity greater than 25 Gb/s up to 40-km standard single-mode fiber (SSMF) [5].

Moreover, DMT has been used for years for digital subscriber line (DSL) applications over copper cables. Unlike wireless communications, DSL channel is time invariant with stationary noise. These characteristics enable DMT bit loading to optimally adapt the transmission capacity to the communication medium features, satisfying the operator request of more flexible networks. With respect to current standardized PONs, where bit-rates are fixed, and all transceivers are designed for maximum rate under worst case channel conditions a network employing link adaptation could offer several advantages such as significant gain in the network capacity, flexibility to adapt to high peak user rates and a more efficient usage of the network resources including energy consumption [6]. Recent works on flexible modulation

This work is funded by the EU H2020 project PASSION under Grant Agreement 780326.

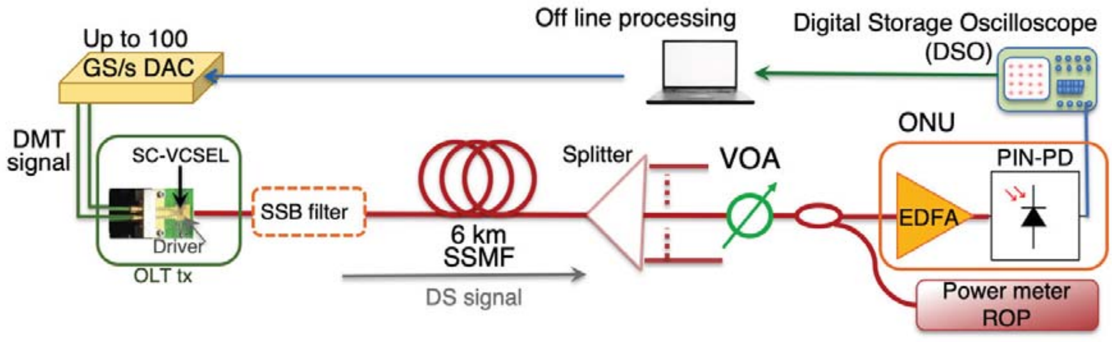

Fig.1 Emulated PON based on DM DMT VCSEL transmitter: experimemtal set up.

schemes in PONs focus on pulse amplitude modulations (PAMs) [6, 7] and a few works on adaptive modulation either based on DD or coherent detection have been done [8, 9].

In this paper we propose to exploit fixed wavelength short cavity (SC) VCSELs, reliable both in O and C bands and providing high modulation bandwidths [10, 11] to realize PON transmitters exploiting direct DMT modulation for the line rate of 50 Gb/s. The advantages of this solution are presented in Section II, also with considerations regarding the energy effectiveness.

In Section III we experimentally evaluate the performance of currently available VCSELs in the third window for back-to-back (BTB) and in case of 100 ps/nm of cumulated chromatic dispersion (CD). As 50G-PON downstream (DS) wavelength should be in the O-band (around 1342±2nm [12]), the CD considered in our experimentation is higher than the accumulated CD (around 74 ps/nm) typical of PON reach of 20-km SSMF. We analyze direct DMT modulation both in dual sideband (DSB) and single sideband (SSB) configurations.

In Section IV we compare the obtained results with simulations realized by developing a transmission model including the electro/optical and chirp transfer functions of the VCSELs. We use the developed simulator to foresee the performance in 50G PON of transmitters based on next-generation VCSELs under development.

In Section V we show the capabilities of direct DMT modulation to increase the data rate in IM/DD PONs with the use of standard hard-decision (HD) forward error correction (FEC). Statistics regarding a commercially deployed PON is considered to evaluate the impact of the proposed transmitter on the flexible PON aggregated capacity.

II. VCSEL BASED TRANSMITTER FOR DMT MODULATION

In order to design a low-cost and energy-efficient transmitter able to match all the requirements of a flexible 50G PON, VCSEL sources, characterized by light emission normal to the semiconductor layer structure, can be exploited. With respect to traditional edge-emitting semiconductor, such as DFB lasers, in case of VCSEL simple and cost-effective on-wafer testability is possible. In the short wavelength region of up to ~1-µm, GaAs VCSELs are massively employed in high-speed data communications in local and storage area networks (LANs and SANs), as well as for computer and datacom applications. About all VCSELs exploited for data links are multi-transverse mode (MM) sources, without specific control of mode forming dynamics and mode polarization. MM VCSELs are compatible with inexpensive optical coupling into multi-mode fibers (MMFs). Owing to typical spectral changes and mode hopping, the exploitation of MM VCSELs in short-reach connections is not so suitable. By exploiting single-mode (SM) emission, very high bit rates have been achieved with short-wavelength VCSELs, even up to 60 Gb/s in case of on-off keying (OOK) operation but limited to hundreds of meters of SSMF propagation [13].

On the other side, emission in the O- and C-band is assured by long-wavelength VCSELs in InP, based on a laser design featuring a dielectric bottom mirror, a buried tunnel junction (BTJ) for the current confinement, a gold substrate acting as a heat sink, a multi quantum well (MQW) active region and an optimized waveguide design. SM operation is guaranteed by transverse waveguide structure, with high sidemode suppression ratios and polarization stable output. SC VCSELs are designed to achieve large modulation bandwidths, reducing the effective cavity length and the photon lifetime in the VCSEL cavity. Moreover, high relaxation-resonance frequencies, and reduced parasitic effects guarantee high-speed modulations [14]. Both O and C band SC devices present a current aperture of about 5 µm and an effective cavity length of 2.5 µm leading to modulation bandwidths up to 20 GHz with relative intensity noise below -140 dB/Hz [10, 11]. Very high rates transmissions have been already demonstrated, i.e. 100-Gb/s polarization-division multiplexed (PDM) PAM4 transmission over 400 km, also for 1.5-µm InP VCSELs [15]. Long-wavelength VCSELs features very efficient power consumptions with output optical powers up to 7 dBm at bias currents in the range of 5-10 mA.

Although long-wavelength VCSELs do not show commercial mass production, they appear very promising for applications in medium-reach connections employing SSMFs, where low cost and power consumption are mandatory. In order to exploit all the benefits of the long-wavelength VCSELs for high data rate transmission, direct DMT modulation can be used. DMT [16] is an effective modulation technique for stationary media, employed for decades in copper links, but also appropriate for fiber-based PON connections. Thanks to its water-filling nature, DMT can distribute the power and the modulation according to the spectral transfer function of the transmission link. The signal-to-noise ratio (SNR) of each subcarrier is estimated during the training phase, and a suitable bit loading is performed to maximize the whole transported capacity with respect to single-carrier modulation performance. DMT modulation shows advantages for the service provider, not only in terms of performance, but also in terms of flexibility and compatibility. Flexible shaping of the transmitted signal spectrum as a function of the channel is assured. For example, in case of DSL applications, any operation frequency band can be implemented by employing the same hardware and applied both to private and public networks for both symmetric and asymmetric connections. In case of optical networks, flexibility allows to optimize the capacity in reaches characterized by higher losses or dispersion impairments, while performance can be dramatically increased in case of very short links [17].

In this work, we take into account InP long-wavelength SC VCSEL sources realized by VERTILAS company, optimized to emit in the O-band or in the C-band. In the experimentation we employed already available 17-GHz bandwidth VCSELs, but in the frame of the European H2020 project PASSION VCSELs with a higher bandwidth (up to 25 GHz) are being developed [18]. The use of simple direct DMT modulation of the VCSEL avoids the need of an external modulator, while employing very low bias current (about 9 mA) and modulation depth achievable with linear drivers commercially available for short-wavelength PAM4 VCSEL applications. Considering an equivalent modulation capacity of 50 Gb/s achievable by the DMT modulation, VCSEL energy consumption per bit is about 0.7 pJ/b, while the power dissipation of the above drivers supporting signaling rates up to 56Gb/s is 230 mW. Hence, the total energy consumption per bit is about 5.3 pJ/s, that is very low compared to the consumption of standard DFB laser sources and silicon photonics chips for external modulation [19]. These values confirm the capabilities of InP VCSEL technology combined to DMT direct modulation for implementing alternative transmitters for 50G PON applications, also from the point of view of sustainability in terms of power consumption.

III. Experimentation

We evaluated the performance of the transmitter based on DM VCSELs by emulating a PON, depicted in the experimental setup of Fig. 1. We tested both DSB DMT and SSB DMT modulations in order to compare their achievements with particular regard towards the impact of CD. The available VCSEL emits at 1533.5 nm, but shows the same characteristics in terms of chirp and E/O bandwidth of 1.3 µm devices, thus to accumulate a dispersion equivalent to 20-km SSMF transmission at 1342 nm (around of 74 ps/nm), a spool of less than 6 km SSMF is needed [12]. The obtained experimental results are also used as benchmarks for the development of a suitable simulation tool as further described in Section IV.

A. Experimental set up

At the optical line terminal (OLT), the transmitter hosts a 17-GHz long-wavelength SC VCSEL, which is directly modulated by a DMT signal generated by a Micram 100-GS/s digital to analog converter (DAC) with 35-GHz electrical bandwidth and 6-bit vertical resolution, through a 25GHz electrical driver. The DMT signal is calculated by Matlab® and is composed by 256 sub-carriers in 20 GHz range, i.e. the sub-carrier spacing is 78.125 MHz. A cyclic prefix (CP) of about 2.1% of the symbol length is added. The bias current is set to 9 mA, with an optimized modulation amplitude of 10 mA and 8 mA for DSB DMT for SSB DMT modulations respectively. SSB modulation is performed by exploiting a programmable optical filter (Finisar WaveShaper 4000S) featuring a super-gaussian transfer function [20], which is detuned by 8 GHz with respect to the signal carrier, for removing the low-frequency signal sideband.

The BTB performance is compared with the results obtained after 6.3-km SSMF propagation, corresponding to a cumulated CD around 100 ps/nm; a variable optical attenuator takes into account further ODN losses and varies the received optical power (ROP). At the ONU end, we used a preamplified receiver, composed by an Erbium-doped fiber amplifier (EDFA) followed by a 25-GHz PIN photodiode. However, the exploited configuration can be easily replaced by a 25G avalanche photo diode (APD) working in the second window.

The received signal is acquired by a Tektronix real-time oscilloscope (DPO 73304DX) with 8 bits vertical resolution, 100 GS/s and 33-GHz electrical bandwidth. Off-line processing provides digital symbol synchronization, CP removal, sub-carriers phase recovery, equalization and demodulation. Finally, the bit error rate (BER) count is obtained.

B. Experimental results

The DMT modulation allows to adapt the modulation of each subcarrier to the channel characteristics, which are at first estimated by transmitting a probe DMT signal with uniform QPSK loading, providing the SNR of each sub-carrier. The measured SNRs act as a feedback of the communication channel conditions and, hence, are exploited for performing Chow's algorithm, i.e. a suitable bit- and power-loading procedure for obtaining a good approximation of the highest bit rate achievable by the transmission system [21]. As target BER, we selected $4.62 \cdot 10^{-3}$, corresponding to the pre FEC BER of advanced HD FEC codes with 7% overhead [11].

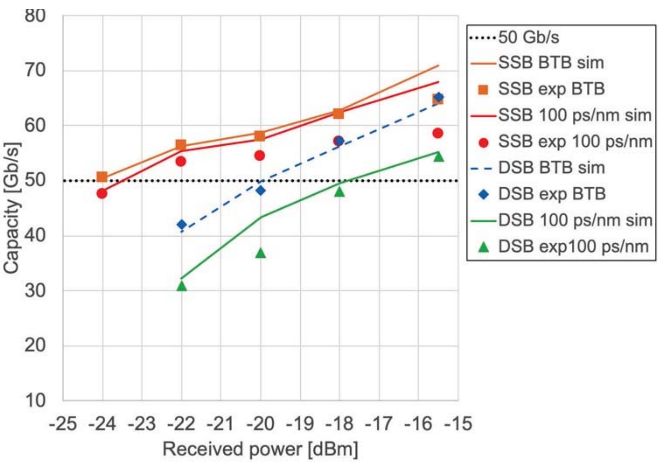

Fig. 2 Comparison between experimental results (full markers) and simulations (lines). Transmitted capacity as a function of the received optical power for SSB DMT (orange and red) and DSB DMT (blue and green), in BTB (squares and diamonds) and after 100ps/nm cumulated CD (circles and triangles).

Fig. 2 shows the measured transmitted capacities as a function of the ROP for BTB and 100 ps/nm cumulated CD. Firstly, we considered the BTB situation, in order to check the performance of the different modulation conditions with respect to the ROP. Even with no SSMF propagation, SSB modulation shows a better performance: in fact, although at the highest received power DSB capacity is slightly greater than the SSB one, the convenience of SSB modulation (orange squares) appears from -18 dBm ROP, permitting to achieve 50 Gb/s capacity even for -24 dBm ROP, while DSB modulation (blue diamonds) is limited to -20 dBm ROP. Then, to assess the robustness of the proposed modulation conditions, we analyzed the performance after 6.3-km SSMF propagation. As expected, due to SSB resilience towards CD, for 100 ps/nm cumulated dispersion conditions, SSB modulation still shows better performance and achieves a sensitivity to target 50 Gb/s transmission around -23 dBm, while DSB modulation requires -18 dBm. Considering that the VCSEL output power ranges around 7 dBm, the PR30 class (29-dB ODN losses) can be successfully supported for SSB modulation (red circles) allowing more than 20 km propagation in O-band. On the other hand, for DSB modulation (green triangles) the PR30 class allows a capacity around 30 Gb/s.

IV. Performance evaluation of 50G PON

The previous measurements have been employed to implement and verify a simulation tool able to predict the performance of transmitters based on new generation long-wavelength SC VCSELs, currently under development [18].

A. Simulation tool

Our simulations are obtained developing a modeling tool based on Matlab™ which includes all the transmitter, propagation, and receiver blocks. Specifically, the DM VCSEL is modeled considering both the intrinsic modulation properties and the extrinsic device parasitic components. The overall electrical modulation frequency response is described by the relaxation resonance frequency, the intrinsic damping factor and the parasitic cut-off frequency [22]. In particular, the setting of these parameters allows to model the current SC VCSEL employed in the experimentation, providing a modulation frequency bandwidth of 17 GHz, and the next generation SC VCSEL which are being developed with a target frequency bandwidth of more than 20 GHz. The VCSEL is also characterized by its linewidth, which is set to 5 MHz, as actually measured in current SC devices. Finally, DM is performed by varying the applied current: setting a bias current and adding a variable modulation. This influences the chirp amount associated with DM and characterized by the linewidth enhancement factor, α, and by the laser-specific adiabatic constant related to thermal effects, κ. The α factor impacts on both the chirp transient and adiabatic components, while the κ factor influences only the adiabatic chirp. In the simulations the α and κ factor are 3.7 and 1.52×10^{13}, values that were measured for the SC VCSELs under test in Section III [22]. The receiver block is constituted by a pre-amplified 25-GHz PIN PD for the modeling of Section III measurements, characterized by a noise equivalent current (NEC) of 40 $pA/\sqrt{Hz}$ and a responsivity of 0.7 A/W; moreover, due to the presence of the EDFA, the optical signal to noise ratio (OSNR) is varied accordingly to the input (i.e. received) optical power. On the other hand, for the simulation of the performance of next generation VCSEL-based transmitters, we employed in the receiver block a simple 25 GHz APD: these devices are in fact becoming available in the market and will likely be hosted in ONU transceivers [3]. Si-Ge APDs can achieve a gain-bandwidth product of 300 GHz, which at 25 GHz allows a gain of 12, with NEC around 20 $pA/\sqrt{Hz}$ and responsivities close to 0.7 A/W [23, 24].

B. Simulation comparison with measurements

As in the actual measurements, the DMT signal is composed by 256 sub-carriers in 20 GHz range, with a 2.1% CP; the bias current is set to 9 mA, with a modulation amplitude of 10 mA and 8 mA for DSB DMT for SSB DMT modulations respectively. The SSB signal is obtained by detuning of 8 GHz a 21-GHz full-width half-maximum (FWHM) super-gaussian filter in order to select half of the 20-GHz DMT DSB spectrum, while preserving the optical carrier. As previously described, both the ROP and the OSNR are varied during simulations according to the performed measurements. The obtained results are shown in Fig. 2 as lines matching the color of the measured capacities, represented by the markers, for BTB and 100 ps/nm CD. In both transmission conditions there is a very good agreement between simulations and experimental results, although for high ROP values the simulations slightly overestimates the obtained capacity.

C. Performance evaluation of transmitters based on next generation SC VCSEL

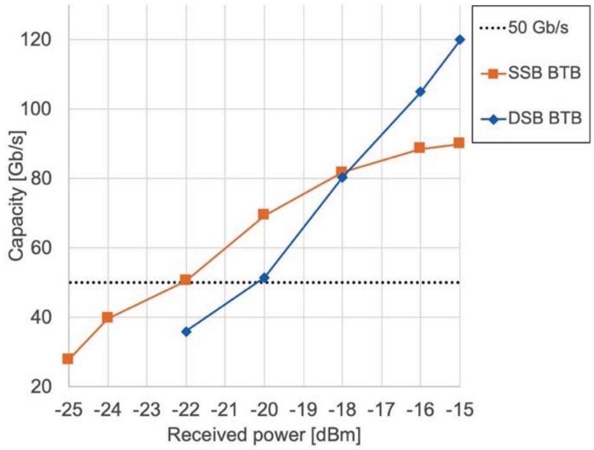

Fig. 3 BTB capacity as a function of the received optical power for SSB DMT (orange squares) and DSB DMT (blue circles).

After validating the simulation tool, we employed it in order to evaluate the performance of transmitters based on next generation O-band SC VCSEL in case of advanced HD FEC with 7% overhead providing a pre-FEC BER of $4.62 \cdot 10^{-3}$. The DMT signal is the same of Section IV-B. As previously stated, in this case the VCSEL parameters were set in order to achieve a modulation bandwidth of 20 GHz, while the exploited receiver was a 25-GHz APD. The bias current was 9 mA, while the modulation amplitudes were separately optimized for DSB and SSB modulations in the case of 105 ps/nm accumulated dispersion and were set respectively to 14 mA and 12 mA.

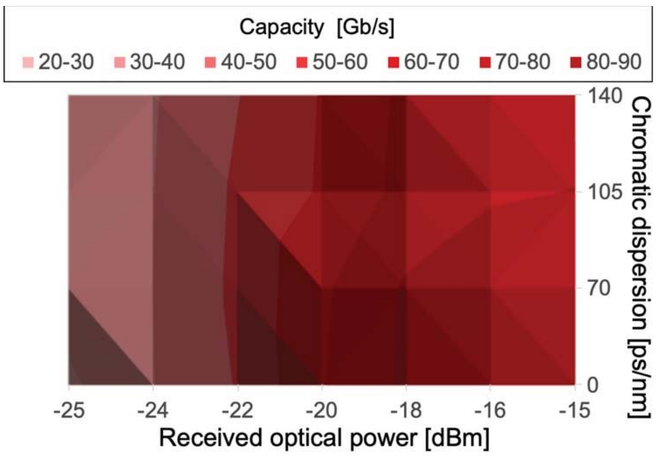

Fig. 4 Contour plot of the SSB DMT transmission capacity as a function of received power and cumulated chromatic dispersion. Capacity > 50 Gb/s (red sectors) capacity between 28 Gb/s and 50 Gb/s (pink sectors).

Moreover, in the case of SSB modulation the filter detuning was optimized to 10 GHz. In both cases the optimization was driven by the provision of the highest capacity. Fig. 3 shows the results for the obtained capacity as a function of the ROP in BTB: DSB DMT outperforms SSB DMT for ROP higher than -18 dBm, but for lower ROP SSB DMT shows better performance and allows more than 50 Gb/s capacity for received powers higher than -22 dBm. At bias current around 10 mA the VCSEL output power is around 7 dBm allowing to support PR 30 link budget. If we include the impact of CD on the transmission of the DM signals the better performance of SSB DMT are even more evident. As expected, in fact, SSB DMT presents a higher resilience towards CD; the contour plot of Fig. 4 demonstrates that for ROP higher than -22 dBm and for CD up to 140 ps/nm (corresponding to the dispersion of 40 km SSMF) SSB DMT modulation allows a transmission capacity higher than 50 Gb/s (red sectors), while between -25 dBm and -22 dBm (pink sectors) the capacity ranges between 28 Gb/s and 50 Gb/s.

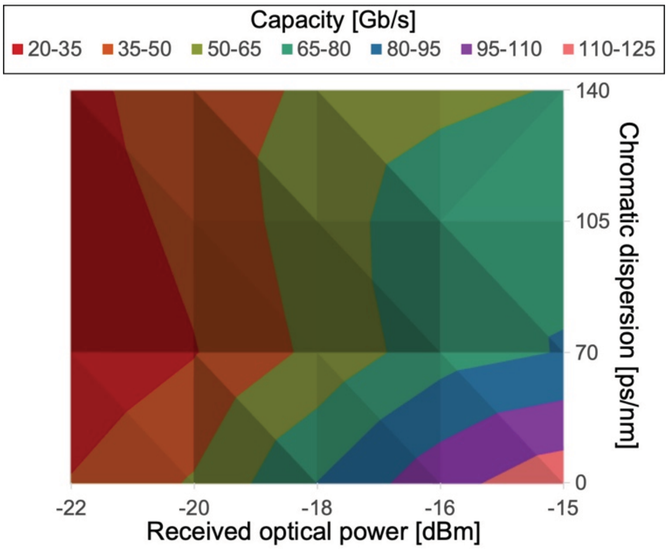

Fig. 5 Contour plot of the DSB DMT transmission capacity as a function of received power and cumulated chromatic dispersion. Capacity between 20 Gb/s and 50 Gb/s (red-orange sectors) capacity > 50 Gb/s (green-blue-purple sectors).

The impairments due to CD are otherwise more significant for DSB DMT, allowing a capacity higher than 50 Gb/s up to 140 ps/nm for ROP higher than -19 dBm (green-blue-purple sectors); however for CD lower than 70 ps/nm (corresponding to 20 km SSMF) and ROP higher than -18 dBm more than 80 Gb/s capacity can be achieved.

The motivation of this behavior can be explained by comparing Fig. 6 for DSB DMT and Fig. 7 for SSB DMT, where from a) to f) the received electrical spectrum, the bit loading, the BER and SNR per subcarrier and examples of received constellations are shown. In particular if we look at Fig. 6 d) a dip in the SNR can be seen around 10 GHz; this is consistent with the frequency dips present in the fiber channel transfer function due to the interplay between chirp and CD. Although for frequencies higher than the dip the SNR increases allowing to use for example 8-QAM in the last subcarriers the overall performance is lower than the SSB DMT. With the SSB spectrum in fact no dips for the interplay between chirp and CD are present, i.e. the SNR constantly decreases for higher frequencies.

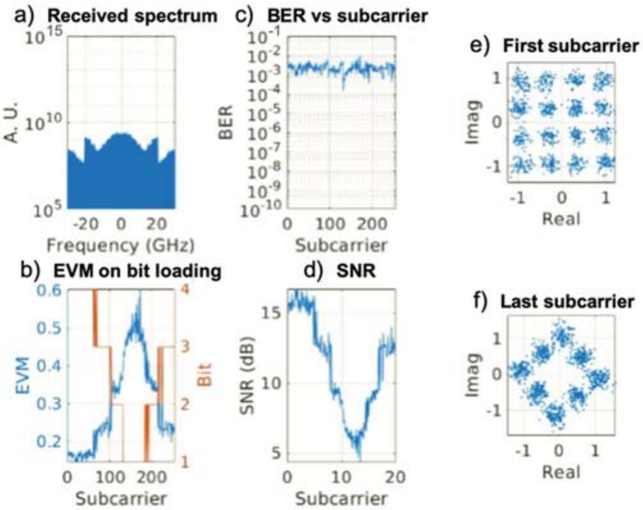

Fig. 6 (a–f) DSB DMT transmission with ROP of -18 dBm and capacity of 53.7 Gb/s: (a) Received electrical spectrum; (b) Bit loading and corresponding EVM; (c) BER per subcarrier; (d) Bit-loading SNR; (e,f) Examples of received constellations.

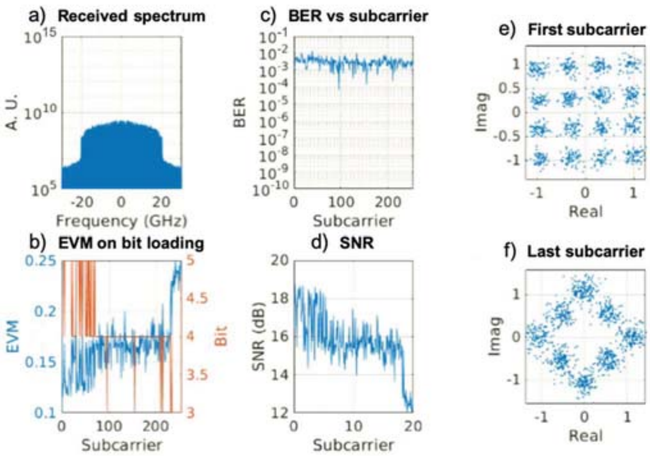

Fig. 7 (a–f) SSB DMT transmission with ROP of -22 dBm and capacity of 52.2 Gb/s: (a) Received electrical spectrum; (b) Bit loading and corresponding EVM; (c) BER per subcarrier; (d) Bit-loading SNR; (e,f) Examples of received constellations.

V. Discussion

In order to estimate the improvement of the throughput of flexible PONs employing the proposed VCSEL-based transmitter exploiting DM DMT, it is necessary to consider the statistical distribution of the ROP within one typical PON deployment. For this purpose, we fitted the statistics of a data set of a GPON deployment with a normal distribution [6]. Fig. 8 shows the number of ONUs with respect to the corresponding ROP: in particular, each band defines the ROP range corresponding to one standard deviation. In order to understand the improvement of the throughput with respect to the fixed-rate transmission condition, we use Fig. 8 percentages and simulative results reported in Fig. 4 and Fig. 5 to calculate the overall aggregated data rates. For 20-km SSMF (around 70 ps/nm CD), in case of SSB the flexible VCSEL-based PON exploiting DMT has a throughput of ~ 65 Gb/s, i.e. a 30% increase with respect to the fixed-rate 50G PON. In the same way, in case of DSB, the flexibility provides ~ 35 Gb/s, with a 40% increase with respect to fixed-rate 25G PON.

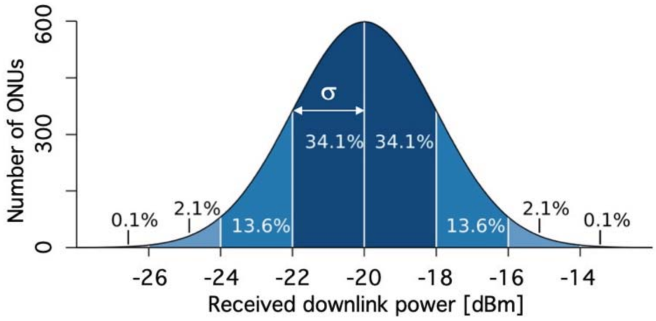

Fig. 8 Normal distribution fitting the ONU received optical power, according to [6].

VI. Conclusions

In this paper we investigate flexible PON transmitters based on the exploitation of the innovative long-wavelength SC VCSEL technology combined with direct DMT modulation, both in SSB and DSB configurations. The experimentation based on already available VCSELs in the third window shows a good robustness to CD, enabling also 50G operation for PR30 class in case of SSB up to 100 ps/nm. Suitable simulations validated by the experimentation have allowed to evaluate the performance of DMT transmitters based on next-generation O-band VCSELs. DMT modulation, providing link adaptation, offers several advantages with respect to single-carrier based fixed-rate PON such as significant increase in the network capacity. Thanks to a statistical analysis of a typical deployed PON, we estimated the flexible PON throughput increase, which allows an efficient usage of the network resources in terms of energy consumption, assured also by the exploited VCSEL technology.

Acknowledgment

The authors thank Federico Lipparini and Micram for the fruitful discussions and for the sponsorship.

References

[1] Frank J. Effenberger, "PON standardisation status and future prospects" in European Conference on Optical Communications ECOC 2019, Dublin, paper M.2.F.1

[2] "40-gigabit-capable passive optical networks 2 (NG-PON2): Physical media dependent (PMD) layer specification: Amendment 1," ITU-T Recommendation G.989.2Amd1, Apr. 2016.

[3] V. E. Houtsma, D. T. van Veen, "Optical strategies for economical next generation 50 and 100G PON" in Optical Fiber Communication Conference (OFC) 2019, San Diego, CA, paper M2B.1 (2019).

[4] T. Takahara, T. Tanaka, M. Nishihara, Y. Kai, L. Li, Z. Tao, and J. C. Rasmussen, "Discrete multi-tone for 100 Gb/s optical access networks," in Optical Fiber Communication Conference (OFC) 2014, San Francisco, CA, paper M2I.1, (2014).

[5] Gatto, P. Parolari, C. Neumeyr, P. Boffi, "Beyond 25 Gb/s directly-modulated widely tunable VCSEL for next generation access network," in Optical Fiber Communication Conference (OFC) 2018, San Diego, CA, paper Th1E.2, (2018).

[6] R. V. Der Linden, N. C. Tran, E. Tangdiongga and A. M. J. Koonen, "Increasing flexibility and capacity in real PON deployments by using 2/4/8-PAM formats," in IEEE/OSA Journal of Optical Communications and Networking, vol. 9, no. 1, pp. A1-A8, Jan. 2017.

[7] D.T. van Veen, Vincent E. Houtsma, "Flexible 50G PON based on multi-rate PAM and CAP-4 with user interleaving" in European Conference on Optical Communications ECOC 2019, Dublin, paper M.2.F.5

[8] H. Kimura, K. Asaka, H. Nakamura, S. Kimura, and N.Yoshimoto, "First demonstration of energy efficient IM-DD OFDM-PON using dynamic SNR management and adaptive modulation," in Proc. European Conf. on Optical Communication (ECOC), 2013, paper We.4.F.5.

[9] F. Vacondio, O. Bertran-Pardo, Y. Pointurier, J. Fickers, A. Ghazisaeidi, G. de Valicourt, J.-C. Antona, P. Chanclou, and S. Bigo., "Flexible TDMA access optical networks enabled by burst-mode software defined coherent transponders," in Proc. European Conf. on Optical Communication(ECOC), 2013, paper We.1.F.2

[10] A. Malacarne, C. Neumeyr, W. Soenen, F. Falconi, C. Porzi, T. Aalto, J. Rosskopf, J. Bauwelinck, and A. Bogoni, "Optical transmitter based on 1.3μm VCSEL and SiGe Driver Circuit for Short Reach Applications and beyond", J. Lightwave Technol., 2018, **36**, pp.1527-1536.

[11] R. Rodes, M. Müeller, B. Li, J. Estaran, J. B. Jensen, T. Gruendl, M. Ortsiefer, C. Neumeyr, J. Rosskopf, K. J. Larsen, M.-C. Amann, and I. T. Monroy, "High-speed 1550 nm VCSEL data transmission link employing 25 GBd 4-PAM modulation and hard decision forward error correction," J. Lightwave Technol., 2013, **31**, pp. 689-695.

[12] M. Tao, J. Zheng, X. Dong, K. Zhang, L. Zhou, H. Zeng, Y. Luo, S. Li, and X. Liu, "Improved dispersion tolerance for 50G-PON downstream transmission via receiver-side equalization," in Optical Fiber Communication Conference (OFC) 2019, San Diego, CA, paper M2B.3.

[13] N. Ledentsov, L. Chorchos, M. Agustn, N.N. Ledentsov, and J.P. Turkiewicz, "850 nm single-mode VCSEL for error-free 60 Gbit/s OOK operation and transmission through 800 m of multi-mode fiber," OFC 2019, PDP, 2019

[14] M. Mueller, W. Hofmann, T. Grundl, M. Horn, P. Wolf, R. D. Nagel, E. Ronneberg, G. Bohm, D. Bimberg, and M.-C. Amann et al., "1550 nm high speed short-cavity VCSELs," IEEE J. Sel. Topics Quantum Electron., 2011, 17, (5), pp. 1158–1166.

[15] C. Xie, S. Spiga, P. Dong, P. Winzer, A. Gnauck, C. Greus, M. Ortsiefer, C. Neumeyr, M. Muller, and M.C. Amann, "Geenration and transmission of 100-Gb/s PDM 4-PAM using directly modulated VCSELs and coherent detection," Proc. OFC 2014, 2014.

[16] R.G. Gallager, "Information theory and reliable communication", Wiley, 1968.

[17] Q. Aldrubi, A. Shalash, et al., "A new out-of-band PSD definition for upstream optional band and its effect on the downstream performance," ANSI contribution T1E1.4/2001-289, 2001.

[18] http://www.passion-project.eu/wp-content/uploads/2019/06/PASSION_D3.4_v1.0.pdf accessed Oct 2019

[19] A. Boletti, P. Boffi, P. Martelli, M. Ferrario, and M. Martinelli, "Performance analysis of communication links based on VCSEL and silicon photonics technology for high-capacity data-intensive scenario," Optics Express, vol. 23, no. 2, pp. 1806-1814, 2015

[20] C. Pulikkaseril, L. A. Stewart, M. A. F. Roelens, G. W. Baxter, S. Poole, and S. Frisken, "Spectral modeling of channel band shapes in wavelength selective switches" Opt. Express, 2011, 19, pp. 8458-8470.

[21] P. S. Chow, J.M. Cioffi, J.A.C. Bingham, "A practical discrete multitone transceiver loading algorithm for data transmission over spectrally shaped channels," IEEE Trans. on Comm., 1995, 43, pp. 773-775.

[22] M. Rapisarda, A. Gatto, P. Martelli, P. Parolari, C. Neumeyr, M. Svaluto Moreolo, J. M. Fabrega, L. Nadal and P. Boffi. "Impact of chirp in high-capacity optical metro networks employing directly-modulated VCSELs" Photonics 2018, 5(4), 51.

[23] M. Nada, T. Yoshimatsu, Y. Muramoto, H. Yokoyama and H. Matsuzaki, "Design and performance of high-speed avalanche photodiodes for 100-Gb/s systems and beyond," in Journal of Lightwave Technology, vol. 33, no. 5, pp. 984-990, 1 March1, 2015.

[24] Z. Huang, C. Li, D. Liang, K. Yu, C. Santori, M. Fiorentino, W. Sorin, S. Palermo, and R. G. Beausoleil, "25 Gbps low-voltage waveguide Si–Ge avalanche photodiode," Optica 3, 793-798 (2016)